Comparison of Heat Transfer Correlations for Cryogenic Engine Thrust Chamber Design

N. Sugathan*
Indian Space Research Organization, Trivandrum 695547, India
K. Srinivasan†
Indian Institute of Science, Bangalore 560012, India
and
S. Srinivasa Murthy‡
Indian Institute of Technology, Madras 600036, India

A comparative study of the correlations available in the literature is made to arrive at an appropriate pair for estimating the coolant-side and hot-gas-side heat transfer coefficients in the thrust chamber of a cryogenic engine. Based on this, the thermal analysis of a supercritical liquid hydrogen cooled engine is carried out. Results are presented for axial variation of heat transfer coefficients and temperature distributions for coolant and exposed wall. Tubular as well as milled channel configurations are considered for coolant flow.

Nomenclature

C	= characteristic velocity, m/s
C_p	= specific heat, kJ/kg K
D	= diameter of cross section, m
D^*	= throat diameter, m
F	= thrust, kN
G	= mass flux, kg/m^2
H	= specific enthalpy, kJ/kg
h	= convective heat transfer coefficient, W/m^2 K
k	= thermal conductivity, W/m K
L	= total length, m
M	= Mach number of flow
$\dot{m}$	= mass flow rate, kg/s
P	= pressure, bar
Pr	= Prandtl number
Q	= heat quantity, kW
q	= heat flux, kW/m^2
R	= radius of curvature, m
Re	= Reynolds number
r_c	= radius of curvature of throat section, m
S	= radiation shape factor
St	= Stanton number
T	= temperature, K
t	= exposed wall thickness, m
V	= sea level nozzle exit velocity, m/s
x	= axial distance, m
Δx	= incremental distance, m
ϵ	= emissivity factor
μ	= absolute viscosity, kg m/s
ρ	= density, kg/m^3
σ	= Stephan-Boltzmann constant, W/m^2 K^4
τ	= specific heat ratio
Φ	= factor defined in NAL correlations
ϕ	= factor defined in SB correlations

Subscripts

act	= actual
av	= average
a,w	= adiabatic wall
b	= bulk
c	= coolant
cur	= curvature
c,NAL	= coolant side using NAL-Japan equation
c,H&K	= coolant side using Hess and Kunz equation
c,S&T	= coolant side using Sieder-Tate equation
eq	= equilibrium
ent	= entrance
f	= film
g	= hot combustion gas
g,MB	= hot gas side using modified Bartz equation
g,NAL	= hot gas side using NAL-Japan equation
g,SB	= hot gas side using standard Bartz equation
g,t	= total from hot combustion gases
inj	= injection
o	= stagnation value
ov	= overall
r	= roughness
rad	= radiative
SL	= sea level
t	= total
Vac	= vacuum
w	= wall
w,c	= coolant side wall
w,g	= hot gas side wall
x	= value at axial location
1,2	= successive stations in axial direction

Received Oct. 15, 1989; revision received Feb. 13, 1990; accepted for publication April 27, 1990.

*Engineer SF, Cryogenics Group.
†Assistant Professor.
‡Professor and Head, Refrigeration and Airconditioning Laboratory.

Introduction

THE design considerations for a regenerative cooling system that uses supercritical hydrogen as a coolant for the thrust chamber and its thermal performance are discussed in this paper. On the coolant side, two geometries of the coolant passage are considered. They are the brazed tubular and the milled channel configurations. Specifications and the configuration of the liquid oxygen-liquid hydrogen (LOX-LH2) cryogenic engine considered here have been arrived at using the information on similar types of cryogenic engines available in literature.[1-7]

To arrive at a proper design procedure for such an engine, it is imperative that thermal modeling of the thrust chamber be

carried out. Since gas is a high-temperature mixture of the products of combustion, it is necessary to consider all of the three modes of heat transfer on the gas side.

In addition to the heat transfer coefficient on the coolant and hot gas sides, the variation of thermal conductivity of the wall of thrust chamber must also be considered. The problem is complicated when one considers the entire section of the thrust chamber of the rocket engine and the fact that supercritical hydrogen is heated up from about 25 to 350 K. In this region, it is well known that the properties of hydrogen change quite widely. In noncryogenic liquid propulsion systems, stainless steel (SS) has been used as a construction material. However, in the case of cryogenic engines, with the thermal conductance of SS being quite low, copper and nickel flow passages have been recommended.[4,8,9]

Mainly three sets of heat transfer correlations available in literature[9-11] have been used by different engine developing agencies for analyzing the thermal performance. However, when these correlations were used in the present studies for predicting the thermal performance, the results showed a considerable variation. To arrive at an appropriate set of correlations, the published temperature data from experimental engines[6,9] were used for comparison. The correlations that most closely matched the experimental data were used in the thermal analysis. However, it should be emphasized that this assumption must be validated through more detailed experiments planned in the next phase of the present studies.

Design Criteria

Design of the coolant passages and the coolant-jacket structure should, in an ideal case, satisfy the following criteria:

1) Provide adequate cooling of the thrust chamber with minimum pressure drop.

2) The hot exposed wall temperature shall be well within the safe working temperature of the material.

3) The material should be amenable to standard fabrication techniques.

4) The material should be lightweight.

The two thrust chamber coolant-passage configurations that are considered in this study are of the tubular and milled channel type. It is seen that for higher heat flux and high-pressure applications, the channel-wall-type thrust chamber will be advantageous from the point of view of less weight and higher margin for a maximum possible heat flux. Maximum heat flux in the proposed engine thrust chamber is found to be in the range of 2.5-3.0 kW/cm^2 for which case the brazed tubular-wall thrust chamber will be quite safe (up to 6.2 kW/cm^2). For low- and medium-pressure applications, the tubular-wall thrust chamber will be lighter. An additional advantage is its simplicity and ease of construction. However, for the high-pressure (more than 100 bar) and high heat flux applications, channel-wall-type electroformed copper thrust chamber will be lighter than the brazed tubular-wall type.

The main specifications and the configuration of the engine considered here for study are given in Table 1 and Fig. 1.

Table 1 Configuration of the subscale engine

Expansion area ratio	140
Thrust	10.379 kN
Chamber pressure	36 bar
Nominal firing duration	450 s
Oxidizer (flow rate)	LOX (2.1 kg/s)
Fuel (flow rate)	LH2 (0.35 kg/s)
Thrust-chamber mixture ratio (LOX/LH2) by weight	6
Sea level chamber area ratio	8.46
Characteristic length	84 cm
Contraction area ratio of the nozzle	3.09
Nozzle extension	H2 dump cooled from area ratio 8.46-140
Injector	Coaxial multielement type with 18 elements
Igniter	Centrally mounted electrical type with preburner

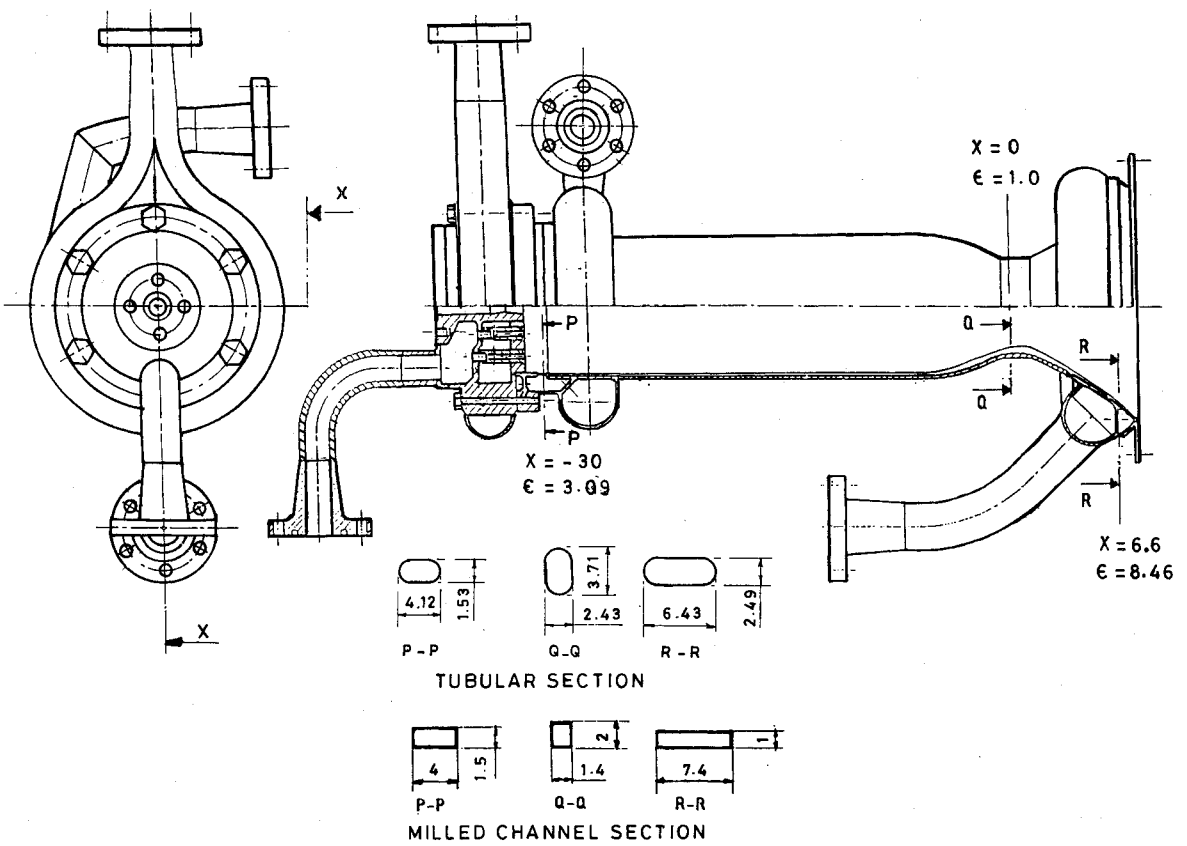

Fig. 1 Thrust-chamber configuration giving coolant-passage dimensions.

Table 2 Correlations for hot-gas-side heat transfer coefficient

1. Standard Bartz Equation[10]:

$$h_{g,SB} = (0.026/D^{0.2})(\mu^{0.2}c_{p,g}/Pr^{0.6})(P/C)^{0.8}(D^*/r_c)^{0.1}(D^*/D)^{1.8}\phi$$

where ϕ is the correction factor for property variation across the boundary layer, given by

$$\phi = [1 + M^2(\tau - 1)/2]^{-0.12}/[0.5 + 0.5(T_{w,g}/T_o) \times \{1 + M^2(\tau - 1)/2\}]^{0.68}$$

2. Modified Bartz Equation[9]:

$$h_{g,MB} = 0.026(G^{0.8}/D^{0.2})(\mu^{0.2}c_{p,g}/Pr^{0.6})(T_o/T_f)^{0.68}$$

3. NAL-Japan Equation[11]:

$$St_g = h_{g,NAL}/(\rho VC_p) = 0.026\, Re_g^{-0.2}Pr^{-0.66}\phi_{inj}$$

where ϕ_{inj} is correction factor for injection, combustion, and mixing, given by

$$\phi_{inj} = A\ W^n$$

where A and n are factors varying with thrust-chamber axial position from injector and W is the injection velocity ratio defined as

$$W = \frac{\text{Velocity of fuel}}{\text{Velocity of oxidizer}}$$

To limit the pressure drop in the coolant passages, excessive velocities should be avoided even though a high velocity is preferable to increase the heat transfer coefficient. Consequently, a velocity limit of 480 m/s (at 227 K) corresponding to a Mach number of 0.405 based on the local conditions is assumed. This corresponds to an available pressure drop of 20% of chamber pressure.

Thermal Model

In the present configuration, the coolant LH2 enters the tubes through a common inlet manifold fitted near the injector side and leaves through the outlet manifold fitted to the divergent portion of the nozzle where the area ratio is 8.46. Coolant flowing through the passages absorbs heat from the wall of the thrust chamber, thereby limiting the exposed wall temperature to a safe value. In the LOX-LH2 engine, using H2 as coolant serves two purposes. First, it limits the temperature of the wall of the thrust chamber. Second, heating H2 to a minimum of 80 K before injection is essential to avoid instabilities[3] in combustion at the injector.

The thermal model adopted for the present study is shown in Fig. 2. Heat transfer at any section of the thrust chamber is predominantly radial since the temperature gradients in the axial direction as well as circumferential direction are comparatively insignificant. Hence, the solution of the problem is simplified to that of one-dimensional steady-state conduction. The wall of the coolant passage separates the combustion gases on one side where the adiabatic wall temperature of the bulk stream is $T_{a,w}$, and the coolant on the other side has a bulk temperature of T_c. Therefore,

$$q_g = h_{g,t}(T_{a,w} - T_{w,g}) = (k_w/t)(T_{w,g} - T_{w,c}) = h_c(T_{w,c} - T_c) \quad (1)$$

The analysis calculates the values of $T_{w,g}$, $T_{w,c}$, and T_c successively at each station along the length of the thrust chamber using the energy conservation Eq. (1) for heat transfer from the combustion product to the coolant across the tube wall. Also,

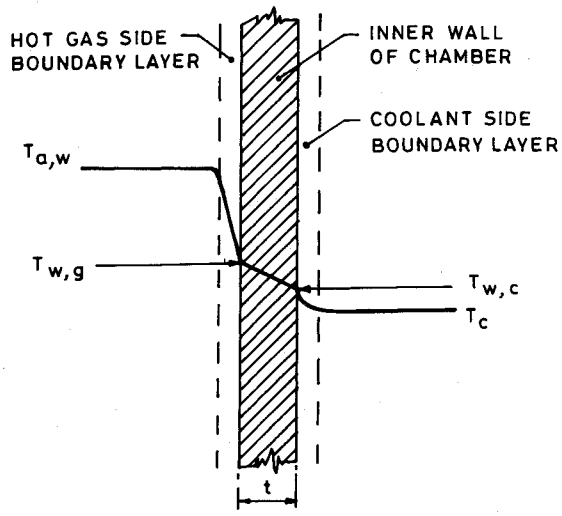

Fig. 2 Heat transfer model.

Table 3 Correlations for coolant-side heat transfer coefficient

1. Sieder-Tate Equation[9]:

$$h_{c,S\&T} = 0.025\ (k/D)\ Re^{0.8}Pr^{0.4}(T_b/T_w)^{0.55}$$

2. Hess and Kunz Equation[14]:

$$Nu_f = (h_{c,H\&K}D/k) = 0.0208\ Re^{0.8}Pr^{0.4}(1 + 0.01457\ \mu_w/\mu_b)$$

3. NAL-Japan Equation[11]:

$$Nu_f = (h_{c,NAL}D/k) = 0.062\ Re^{-0.7}Pr^{0.4}\Phi_{ent}\Phi_r\Phi_{cur}$$

where the entrance factor Φ_{ent} is given by

$$\Phi_{ent} = 1 + (x/D)^{-0.7}(T_w/T_b)^{0.1}$$

and the curvature factor Φ_{cur} is given by

$$\Phi_{cur} = [Re_b(r/R)^2]^{0.02}[1 + 0.32\ \sin\{\pi\sqrt{x/(L + 30\ R)}\}]$$

Roughness factor Φ_r is given by Nunner's equation as

$$\Phi_r = \frac{1 + 1.5\ Pr_b^{-1/6}Re_b^{-1/8}(Pr_b - 1)\zeta}{1 + 1.5\ Pr_b^{-1/6}Re_b^{-1/8}(Pr_b\zeta - 1)}$$

where ζ is the ratio of the rough tube isothermal friction factor to that of a smooth tube.

$$q_g = h_{ov}(T_{a,w} - T_c) \quad (2)$$

where

$$h_{ov} = \frac{1}{(1/h_g,t + t/k_w + 1/h_c)} \quad (3)$$

$T_{a,w}$ is calculated using the following relation[16]:

$$T_{a,w} = T_g + (T_o - T_g)0.91 \quad (4)$$

where the stagnation recovery factor 0.91 is a function of the Prandtl number.

In the above equations, the values of $h_{g,t}$ and h_c have to be determined iteratively through the solution of $T_{w,g}$ and $T_{w,c}$. The hot-gas-side heat transfer coefficient $h_{g,t}$ has a convective component h_g and a radiative component $h_{g,rad}$. Calculation of h_g on the hot gas side is based on three different correlations listed in Table 2. Similarly, the coolant-side heat transfer coefficient h_c also is calculated based on three different correlations given in Table 3. For calculating local heat transfer

coefficients in the case of noncircular passages of the milled channel, the cross section is reduced to an equivalent tube of circular pipe, using the standard definition of hydraulic radius as twice the flow cross section divided by the wetted perimeter. Obviously, this value varies along the axial distance. The effect of the shape of the thrust chamber must be accounted for because the rate of heat transfer downstream of a bend will be more than that upstream of the bend, and it then diminishes to magnitudes characteristic of heat transfer in straight tubes. In the National Aerospace Laboratory, Japan (NAL) equation used by the National Space Development Agency of Japan (NASDA) for their engine heat transfer analysis, a curvature factor Φ has been incorporated to account for the effect of curvature due to bends in the tubes.

Solution

To obtain a complete solution, information on T_o, T_g, and M are required. T_o is calculated based on the oxygen/fuel (O/F) ratio of the propellants. Static gas temperature T_g is calculated as a function of Mach number/area ratio assuming isentropic expansion through the nozzle.[10] Thermophysical properties of combustion products and those of H2 as a function of temperature are obtained from literature.[12,13,15] Monoatomic and diatomic gases are practically transparent to thermal radiation. The maximum emissivity ϵ_g of water is 0.38 at $T_g = 2000°C$ and 0.18 at $T_g = 3100°C$.[16] Also, the emissivity ϵ_w of the exposed wall surface made of pure nickel is about 0.05 at 700–900°C.

As mentioned earlier, the three correlations listed in Table 2 are used in the calculation of h_g. Using the basic radiation equation, the radiative heat transfer coefficient $h_{g,rad}$ between the hot gas and wall surface along the axis of the thrust chamber is determined as

$$h_{g,rad} = S_{w,g}\sigma(\epsilon_g T_g^4 - \epsilon_w T_{w,g}^4)/(T_g - T_{w,g}) \tag{5}$$

It is observed that the contribution of radiation heat transfer is in the range of 5–8% of the convection component in both cases of flow cross sections analyzed here.

For the coolant-side heat transfer coefficient, the NAL equation[13] takes into account the effect of longitudinal curvature of the coolant passage in the critical throat section.

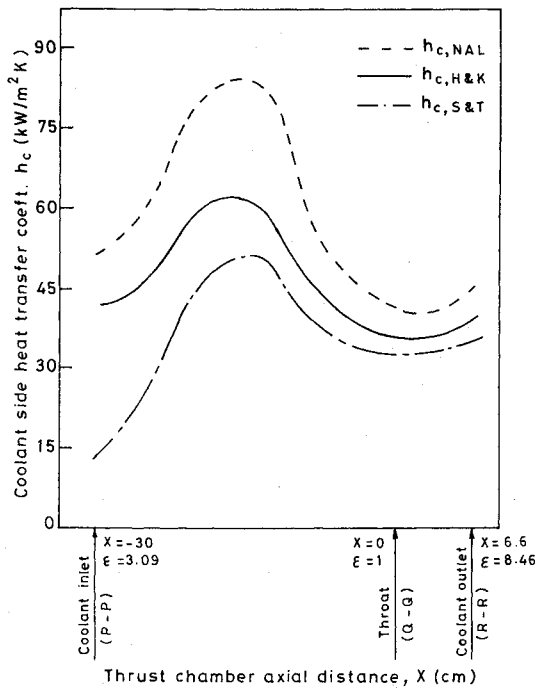

Fig. 3 Comparison of coolant-side heat transfer coefficient for the thrust chamber in Fig. 1.

Since LH2 can be allowed to superheat after phase change, its capacity as a coolant is unlimited. LH2 enters the coolant passage at supercritical pressure (about 50 bar) and reaches a supercritical temperature of 33 K within a short distance from the inlet manifold. Since the coolant in the passage is well above its critical pressure of 12.3 bar, the latent heat transfer and the associated two-phase flow problems are absent during warming up of LH2 into gaseous hydrogen. By considering the nonuniform variation of thermal properties of H2 in the supercritical region, accuracy of prediction of heat transfer parameters can be improved.

Numerical computation at each station starts with determination of the thrust-chamber geometry and local hot-gas flow parameters such as D_x, T_g, M, $C_{p,g}$, and ϕ. Next, the gas-side heat transfer coefficient h_g, adiabatic wall temperature $T_{a,w}$, coolant-side heat transfer coefficient h_c, and the temperature of the coolant T_c are calculated. However, for the first station, i.e., at the entry, T_c is known. Then from Eqs. (1-4), gas-side-wall temperature $T_{w,g}$ is computed. In the calculation of h_g and h_c, the properties are to be evaluated at bulk temperature (e.g., Bartz modified equation). This necessitates assuming a value of $T_{w,g}$ and $T_{w,c}$ to start with. Then at each subsequent iteration, $T_{w,g}$ and $T_{w,c}$ are adjusted in order to match the energy balance. At the next station, the iteration described above is repeated. At each axial location (in the present case 4 cm apart), the enthalpy balance between coolant and hot gas is struck. After computing the parameters such as the local thrust-chamber diameter, $T_{a,w}$, and h_g for the second station, the heat balance to calculate the coolant temperature $T_{c,2}$ at the second station is made as follows:

$$m_c C_{p,c}(T_{c,2} - T_{c,1}) = (\pi/4)(D_1 + D_2)(h_{g,1} + h_{g,2})(\Delta x) \times (T_{a,w} - T_{w,g}) \tag{6}$$

where subscripts 1 and 2 represent the values corresponding to the previous station and station under consideration, respectively. $T_{a,w}$ and $T_{w,g}$ represent the average values of the adiabatic wall and exposed wall temperatures at the two stations under consideration.

The overall energy balance for the sea level portion of the thrust chamber is satisfied as follows:

$$Q_c = \dot{m}_g(H_1 - H_2) + FV \tag{7}$$

Iteration for the station under consideration is repeated using all of the related equations until all parameters, such as $h_{g,2}$, $T_{a,w,2}$, $T_{w,g,2}$, $h_{c,2}$, and $T_{c,2}$, are mutually in agreement for steady-state heat transfer for the section of the thrust chamber. The above computation scheme for heat transfer is continued for the entire length of the thrust chamber.

Results and Discussion

It may be recalled that there are nine combinations corresponding to three correlations each for h_g and h_c. Figures 3 and 4 show the variation of convective heat transfer coefficients along the axial length of the thrust chamber. In the case of the coolant-side heat transfer coefficient, the maximum occurs in the cylindrical portion of the thrust chamber. It drops to a point very close to the throat and slightly increases thereafter up to the outlet. The NAL equation predicts values of heat transfer coefficient which are much higher than the ones predicted by the other correlations. It is found that the hot gas heat transfer coefficient shows a maximum at the throat as per the Bartz-simplified equation, whereas according to the NAL equation, the maximum in h_g occurs slightly downstream of the throat. Furthermore, the latter correlation also predicts a value of the heat transfer coefficient which is considerably lower than that given by the other two correlations. For the nine possible sets of correlations, variations of the hot exposed wall temperature and coolant temperature

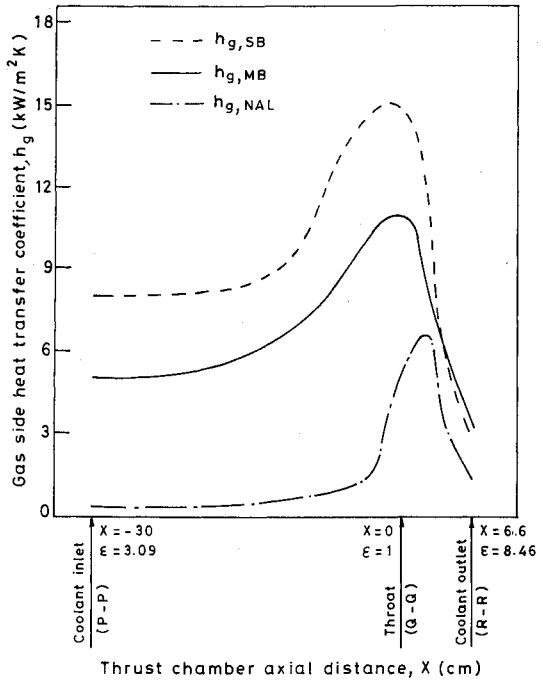

Fig. 4 Comparison of gas-side heat transfer coefficient for the thrust chamber in Fig. 1.

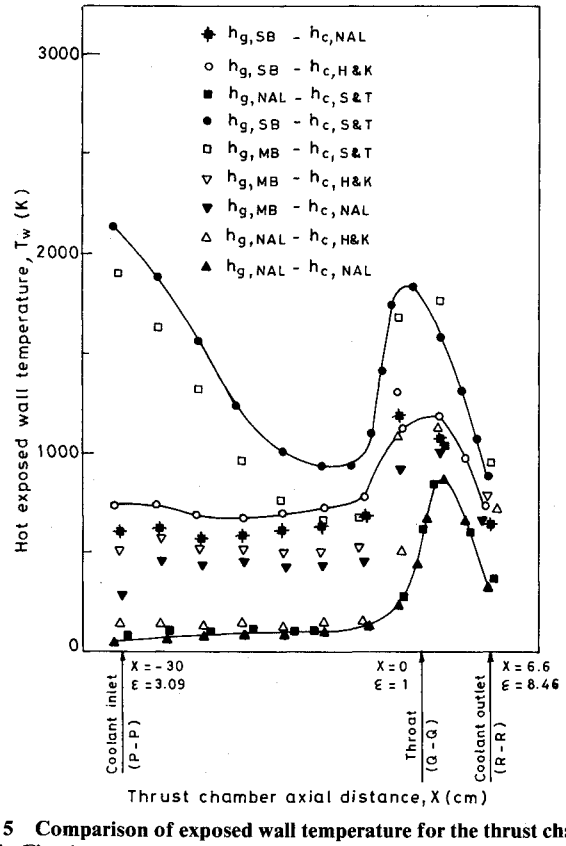

Fig. 5 Comparison of exposed wall temperature for the thrust chamber in Fig. 1.

along the length of the thrust chamber are shown in Figs. 5 and 6. It is apparent that the NAL set of equations predicts a fairly low maximum exposed wall temperature as well as the coolant outlet temperature. The study also reveals that the overall heat transfer coefficient is predominantly governed by the hot-gas-side heat transfer coefficient that is significantly lower than the coolant-side heat transfer coefficient.

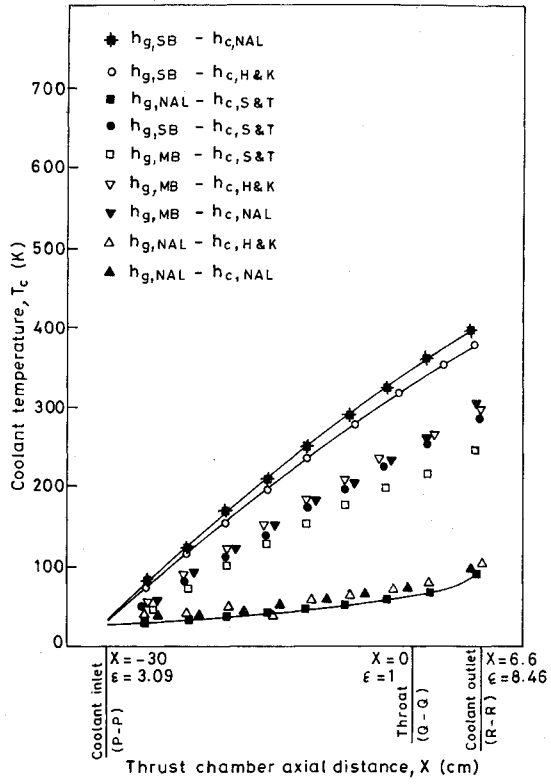

Fig. 6 Comparison of coolant temperature distribution for the thrust chamber in Fig. 1.

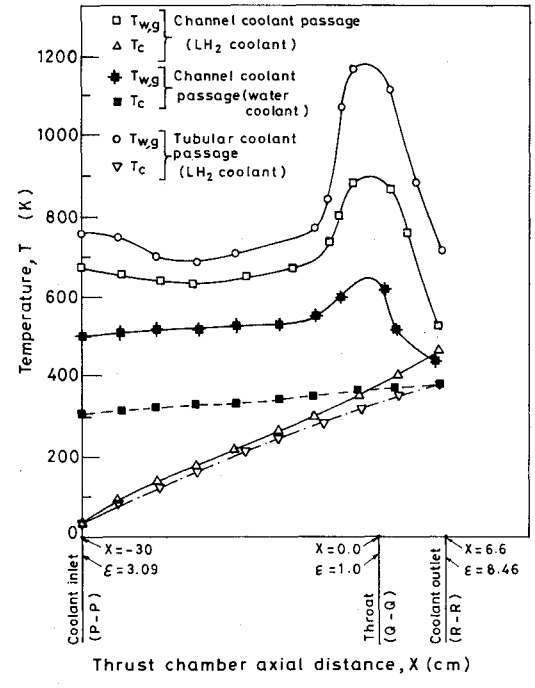

Fig. 7 Variation of wall and coolant temperatures for the thrust chamber in Fig. 1.

In order to arrive at the pair of correlations which should be used, the following procedure has been adopted. The experimental data available from the LE-5 engine[6] for the maximum exposed wall temperature $T_{w,g}$ and the coolant temperature T_c are 900 and 150 K, respectively. Calculations are carried out using all nine possible pairs of correlations for the flow rates reported for the LE-5 engine. The values of $T_{w,g}$ and T_c thus computed are given in Table 4. From these results, it may be observed that the combination of standard Bartz and Hess and

Table 4 Results for the LE-5 engine[6] computed from different pairs of correlations

Correlation pair	$T_{w,g}$, K	T_c, K
$h_{g,SB} - h_{c,NAL}$	823	166
$h_{g,SB} - h_{c,H\&K}$	905	150
$h_{g,SB} - h_{c,S\&T}$	1645	116
$h_{g,MB} - h_{c,NAL}$	781	122
$h_{g,MB} - h_{c,H\&K}$	864	120
$h_{g,MB} - h_{c,S\&T}$	1522	98
$h_{g,NAL} - h_{c,NAL}$	700	39
$h_{g,NAL} - h_{c,H\&K}$	823	40
$h_{g,NAL} - h_{c,S\&T}$	705	38

Kunz correlations yields the values closest to the experimental data. Hence, this pair was chosen for the thermal analysis presented here.

For the engine under study, the variations of exposed wall temperature and the coolant temperature are shown in Fig. 7. The predictions for the brazed tubular thrust chamber show that the maximum exposed wall temperature is about 1200 K in the vicinity of the throat, and the corresponding outlet temperature is about 370 K. In the case of thrust chamber with milled channel coolant passages, the maximum exposed wall temperature is 880 K and the coolant outlet temperature is 480 K.

Conclusions

1) A very wide variation is observed in the coolant and hot exposed wall temperatures of the thrust chamber of a cryogenic engine, when the various correlations available in literature are used for thermal analysis.

2) The heat transfer coefficients on the hot gas side and coolant side obtained, respectively, using the standard Bartz and Hess and Kunz correlations are the most appropriate for thermal design applications.

3) The regenerative cooling method adopted here serves the purpose of cooling the thrust-chamber walls as well as warming hydrogen to temperatures that are acceptable in injectors.

4) The temperature of the thrust chamber can be limited to 1200 K, which is reasonable for tubular thrust-chamber materials, and to 900 K for the copper-milled chamber.

References

[1]Tanat Sugu, N., Nagatomo, M., Akiba, R., and Kuratani, K., "Development Study of LOX/LH2 Propulsion Systems," *Proceedings of the XXXI International Astronautical Congress,* Tokyo, Japan, 1980, pp. 167–178.

[2]Pouliquen, M. F., and Gill, G. S., "Performance Characteristics of HM 7, LOX/LH2 Rocket Engine for the Ariane Launcher," *Proceedings of the AIAA/SAE 14th Joint Propulsion Conference,* Las Vegas, NV, 1978, pp. 1–7.

[3]Harrje, D. T., and Reardon, F. H. (eds.), *Liquid Propellant Rocket Combustion Instability,* NASA SP-194, 1972.

[4]Yanagawa, K., Fujita, T., Miyajima, H., and Kishimoto, K., "High Altitude Simulation Tests of the LOX/LH2 Engine LE-5," *Journal of Propulsion,* Vol. 1, No. 3, 1985, pp. 180–186.

[5]Hirata, K., Denda, Y., Yamada, A., Kochiyama, J., Fujita, T., and Katsuta, H., "Development Tests of LE-5 Rocket Engine," *Proceedings of the 13th International Symposium on Space Technology and Science,* Tokyo, Japan, 1983, pp. 237–242.

[6]Yanagawa, K., Fujita, T., Katsuda, H., and Miyajima, H., "Development of LOX/LH2 Engine LE-5," AIAA Paper 84-1223, June 1984.

[7]Krebs, H. J., "Cryogenic Rocket Propulsion at MBB, Technical Experience," *Proceedings of the 11th International Symposium on Space Technology and Sciences,* Tokyo, Japan, 1975, pp. 129–134.

[8]Seidal, A., "A Completely Electroformed Lightweight Regenerative Thrust Chamber for Cryogenic Rocket Engines," AIAA Paper 74-1183, Oct. 1974.

[9]"Thrust Chamber Cooling Techniques for Space Craft Engines: Final Report," NASA CR-50959, July 1963.

[10]Huzel, D. K., and Huang, D. H., "Design of Liquid Propellant Rocket Engines," NASA SP-125, 1971.

[11]Kumakawa, A., Niino, M., Yatsuyanagi, N., Gomi, H., Sakamoto, H., and Sasaki, M., "A Study of the Cooling of Low Thrust LO2/LH2 Rocket Engine," *Proceedings of the 13th International Symposium on Space Technology and Science,* Tokyo, Japan, 1983, pp. 301–306.

[12]McCarty, R. D., "Hydrogen Technological Survey: Thermophysical Properties," NASA SP-3089, 1971.

[13]Gordon, S., and McBride, B. J., "Theoretical Performance of Liquid Hydrogen with Liquid Oxygen as a Rocket Propellant," NASA TM-5-21-59E, March 1959.

[14]Hess, H. L., and Kunz, H. R., "A Study of Forced Convection Heat Transfer to Supercritical Hydrogen," *Transactions of the ASME, Journal of Heat Transfer,* Vol. 87, No. 2, 1965, pp. 41–48.

[15]Niino, M., Kumakawa, A., Yatsuyanaga, N., and Suzuki, A., "Heat-Transfer Characteristics of Liquid Hydrogen as a Coolant for the LO2/LH2 Rocket Thrust Chamber with the Channel Wall Construction," AIAA Paper 82-1107, June 1982.

[16]Isachenko, V. P., Osipova, V. A., and Sukomel, A. S., "Heat Transfer," Mir Publishers, Moscow, 1977, Chap. 17.